# Orientational Ordering and Intermolecular Interactions in the Rotor-Stator Compounds $C_{60} \cdot C_8H_8$ and $C_{70} \cdot C_8H_8$ Studied under Pressure

**K. Thirunavukkuarasu,[†] C. A. Kuntscher,*,[†] B. J. Nagy,[‡] I. Jalsovszky,[‡] G. Klupp,[§] K. Kamarás,[§] É. Kováts,[§] and S. Pekker[§]**

*Experimentalphysik II, Universität Augsburg, D-86159 Augsburg, Germany, Department of Organic Chemistry, Eötvös Loránd University, Budapest, Hungary, and Research Institute for Solid State Physics and Optics, Hungarian Academy of Sciences, P.O. Box 49, Budapest, Hungary*

Pressure-dependent transmittance measurements on $C_{60} \cdot C_8H_8$ and $C_{70} \cdot C_8H_8$ at room temperature were performed for pressures up to 10 GPa in the mid- and near-infrared frequency range, in order to monitor the vibrational modes of the fullerene and cubane molecules as a function of external pressure. Furthermore, the position of the absorption edge related to intramolecular electronic excitations on the fullerene molecules was studied with increasing pressure. For $C_{60} \cdot C_8H_8$, the anomaly at 0.5 GPa in the pressure dependence of the vibrational modes indicates a pressure-induced orientational ordering transition of the fullerene molecules and the anomaly at 1.3 GPa can be related to fullerene–cubane interaction. In $C_{70} \cdot C_8H_8$, the pressure-induced changes are more pronounced, with a splitting of the cubane modes at the pressures 0.8 and 1.75 GPa. This finding indicates stronger intermolecular interactions in $C_{70} \cdot C_8H_8$ compared to $C_{60} \cdot C_8H_8$, leading to larger distortions of cubane molecules. The energy position of the absorption edge in $C_{60} \cdot C_8H_8$ and $C_{70} \cdot C_8H_8$ shows a nonlinear decrease with increasing pressure. The zero-pressure value of the absorption edge in $C_{60} \cdot C_8H_8$ is larger than that of pristine $C_{60}$ indicating that the cubane molecules reduce the overlap of the $C_{60}$ molecular orbitals. In $C_{70} \cdot C_8H_8$, no shift of the optical absorption edge relative to $C_{70}$ is found, in agreement with this compound being closer to a host–guest system than $C_{60} \cdot C_8H_8$.

## 1. Introduction

The fullerene–cubane molecular crystals $C_{60} \cdot C_8H_8$ and $C_{70} \cdot C_8H_8$, which were synthesized only recently, are the first members of the rotor-stator crystal family.[1] At room temperature, $C_{60} \cdot C_8H_8$ crystallizes in a face-centered cubic (fcc) structure, while $C_{70} \cdot C_8H_8$ forms a body-centered tetragonal (bct) crystal. Static cubane molecules occupy the octahedral voids (elongated octahedron in case of $C_{70} \cdot C_8H_8$) and act as bearings for the rotating fullerene molecules. Although there exists only a weak van der Waals interaction between the fullerene and cubane molecules, they form high-symmetry molecular crystals due to molecular recognition between the convex surface of fullerene and the concave surface of cubane. These novel rotor-stator cocrystals constitute a new family of fullerene derivatives with special intermolecular interactions between the constituents.

On cooling at ambient pressure, $C_{60} \cdot C_8H_8$ undergoes an orientational ordering transition at 140 K, where the rotational degrees of freedom of the fullerene molecules become restricted.[1,2] This transition is accompanied by a change in the crystal structure of $C_{60} \cdot C_8H_8$ from fcc to orthorhombic. $C_{70} \cdot C_8H_8$ undergoes two orientational ordering transitions upon cooling from above room temperature. During the first transition at 390 K, the crystal structure changes from fcc to bct: at room temperature, the free rotation of the $C_{70}$ molecules in $C_{70} \cdot C_8H_8$ is therefore restricted, the basic motion of $C_{70}$ being a uniaxial rotation around the long molecular axis ($C_5$). In addition, the

long axis precesses around the $c$ axis of the tetragonal unit cell. On further cooling below 150 K, the precession of the long axis stops, while the uniaxial rotation of the fullerene molecules persists. This temperature-dependent orientational ordering in $C_{70} \cdot C_8H_8$ is accompanied by a structural phase transition from tetragonal to monoclinic. The cubane molecules are orientationally ordered and remain static in both $C_{60} \cdot C_8H_8$ and $C_{70} \cdot C_8H_8$.

The orientational ordering temperature in these rotor-stator compounds is much lower than in any other fullerene derivative, which was attributed to the expanded lattice and the special rotor-stator interaction facilitating the smooth rotation of the fullerenes.[2,3] Consequently, in fullerene–cubane molecular crystals pressure-induced phenomena are expected to occur at higher pressure compared to pristine $C_{60}$ and $C_{70}$ and other fullerene-derived compounds. Recently, the pressure-induced phenomena in $C_{60} \cdot C_8H_8$ were investigated by pressure-dependent transmittance measurements in the infrared frequency range.[4] It was found that the orientational ordering in $C_{60} \cdot C_8H_8$ indeed occurs at a pressure of about 0.8 GPa, which is significantly higher than for pristine $C_{60}$. Furthermore, high-pressure X-ray diffraction and Raman spectroscopic studies were performed on $C_{60} \cdot C_8H_8$ addressing the issue of pressure-induced polymerization of this compound.[5,6] In these studies, the occurrence of a structural phase transition from cubic to orthorhombic, which is accompanied by the orientational ordering of the $C_{60}$ molecules in $C_{60} \cdot C_8H_8$, was observed at around 0.5 GPa.

Due to the enlarged interfullerene distances in $C_{60} \cdot C_8H_8$ and $C_{70} \cdot C_8H_8$ and the molecular recognition between fullerene and cubane molecules, the fullerene–cubane interaction plays a significant role in addition to the interfullerene interaction. Pressure-dependent spectroscopic investigations enable us to

* Corresponding author. E-mail: christine.kuntscher@physik.uni-augsburg.de.
[†] Universität Augsburg.
[‡] Eötvös Loránd University.
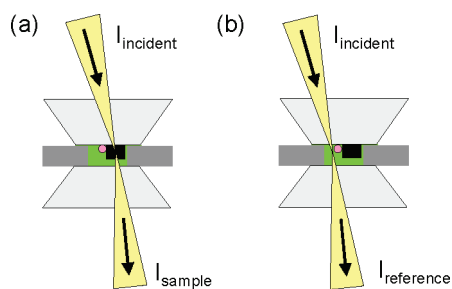[§] Research Institute for Solid State Physics and Optics.

**Figure 1.** Geometries for the transmittance measurements: (a) sample measurement, (b) reference measurement.

study the effect of intermolecular interaction and structural changes on the properties of these materials. Therefore, we carried out a detailed investigation of the optical properties of $C_{60} \cdot C_8H_8$ and $C_{70} \cdot C_8H_8$ under pressure by transmittance measurements in the mid- and near-infrared frequency range. Vibrational (infrared and Raman) spectra of $C_{60} \cdot C_8H_8$ and $C_{70} \cdot C_8H_8$ in both the monomer and polymer phases were thoroughly discussed in a previous publication.[7] In this paper, we present the influence of pressure on the vibrational and electronic properties of $C_{60} \cdot C_8H_8$ and $C_{70} \cdot C_8H_8$ at room temperature.

## 2. Experimental Methods

The $C_{60} \cdot C_8H_8$ and $C_{70} \cdot C_8H_8$ powder samples were synthesized as reported before.[1] The pressure-dependent transmittance measurements were performed at room temperature using a Bruker IFS 66v/S spectrometer with an infrared microscope (Bruker IRscopeII). A diamond anvil cell (DAC) of Syassen-Holzapfel type[8] was used for generation of pressure and the ruby luminescence method was used for pressure determination.[9] The transmission of a mixture of powder sample and the pressure transmitting medium was measured for pressures up to 10 GPa over the frequency range $400-20000$ cm$^{-1}$. The measurements were performed with a resolution of $1-2$ cm$^{-1}$ in the mid-infrared and 8 cm$^{-1}$ in the near-infrared and visible frequency ranges. The quasi-hydrostatic pressure transmitting medium used in the mid-infrared was KCl. Transmittance measurements in the near-infrared (NIR) and visible frequency range were performed using KCl and Ar as pressure transmitting media, in order to check the possible effect of nonhydrostaticity on the pressure dependence of the absorption edge of $C_{60} \cdot C_8H_8$ and $C_{70} \cdot C_8H_8$.

In order to determine the transmittance of $C_{60} \cdot C_8H_8$ and $C_{70} \cdot C_8H_8$ under pressure, the intensity $I_s(\omega)$ of the radiation transmitted by the mixture of the powder sample and the pressure transmitting medium was measured, as illustrated in Figure 1. As reference, the intensity $I_r(\omega)$ transmitted by the pure pressure transmitting medium inside the DAC was used. The transmittance was then calculated according to $T(\omega) = I_s(\omega)/I_r(\omega)$ and the absorbance according to $A = \log_{10}(1/T)$.

## 3. Results and Discussion

**3.1. Vibrational Modes.** The vibrational spectra and the assignment of the normal modes have been extensively discussed in ref 7. Briefly, the spectra consist of the superposition of cubane $T_{1u}$ normal modes, in addition to fullerene $T_{1u}$ modes in $C_{60} \cdot C_8H_8$, and $E_1' + A_2''$ modes in $C_{70} \cdot C_8H_8$, respectively, with no shift of the fullerene modes and a slight redshift of the cubane modes, caused by the high polarizability of the fullerene environment. In the following, we will denote the fullerene and

cubane modes, by F and C, respectively, numbered in the order of increasing frequency.

Figures 2 and 3 show the absorbance spectra of $C_{60} \cdot C_8H_8$ and $C_{70} \cdot C_8H_8$ as a function of pressure. The interference fringes in the spectra are due to multiple reflections of the incident radiation within the DAC. Most of the modes show a pronounced frequency shift and broadening under pressure and can be clearly observed up to the highest applied pressure of about 10 GPa. Furthermore, all the observed pressure-induced changes in the vibrational modes are reversible upon pressure release.

The behavior of the fullerene modes in $C_{60} \cdot C_8H_8$ and $C_{70} \cdot C_8H_8$ under pressure is very similar to that observed in the pristine fullerenes:[10] In $C_{60} \cdot C_8H_8$, the fullerene modes harden with increasing pressure, except for the radial distortion mode at 527 cm$^{-1}$. In $C_{70} \cdot C_8H_8$, most of the fullerene modes shift to higher energies with increasing pressure, except the modes located at 577, 674, 795, and 1586 cm$^{-1}$ which shift to lower energies and exhibit a weak pressure dependence, like in pristine $C_{70}$.[11,12]

For both compounds the vibrational modes of the cubane molecules harden with increasing pressure. Interestingly, the pressure-induced changes for these modes are more pronounced than for the fullerene modes. In particular, in $C_{70} \cdot C_8H_8$ the cubane modes exhibit the signs of splitting in addition to the broadening of the modes. Due to increasing width of the vibrational modes, the split modes are not well resolved and appear as shoulders in the broad absorption lines. The presence of the cubane lines up to 10 GPa proves that copolymerization, as shown to be induced by temperature, light,[7] or high temperature and pressure,[5] does not happen under these circumstances.

For a quantitative analysis of the pressure-induced changes in the absorbance the frequencies of the vibrational modes of $C_{60} \cdot C_8H_8$ and $C_{70} \cdot C_8H_8$ were extracted by fitting with Lorentzian functions. The vibrational modes of $C_{60} \cdot C_8H_8$ and $C_{70} \cdot C_8H_8$ at low pressure (0.5 GPa) and higher pressure (4 GPa) are shown in Tables 1 and 2. The pressure dependence of two selected modes in both compounds are shown up to 10 GPa in Figure 4. The vibrational modes exhibit linear frequency shifts with changes in the slope at certain pressures in the low pressure regime, and the cubane modes in $C_{70} \cdot C_8H_8$ show a three-fold splitting.

For the discussion of our results, we can focus on the pressure range up to 4 GPa, since the major changes occur here (as obvious from Figure 4). The pressure-induced frequency shifts of the vibrational modes of $C_{60}$ and cubane in $C_{60} \cdot C_8H_8$ are plotted in Figure 5. For $C_{60} \cdot C_8H_8$, the anomalies occur at around 0.5 and 1.3 GPa.

The corresponding results of the vibrational modes of $C_{70}$ and cubane in $C_{70} \cdot C_8H_8$ are plotted in Figure 6. Since $C_{70}$ has many infrared-active modes (see Table 2), only those with the strongest pressure dependence are shown in Figure 6. For $C_{70} \cdot C_8H_8$, we observe anomalies in the pressure dependence of these modes at around 0.8 and 1.75 GPa. The anomalies are pronounced for the cubane modes, while they are less obvious for the $C_{70}$ modes.

It is interesting to compare the results of $C_{60} \cdot C_8H_8$ with the pressure–temperature ($P-T$) phase diagram of pristine $C_{60}$, in order to get insight into the possible nature of the observed anomalies in $C_{60} \cdot C_8H_8$. The orientational ordering transition in $C_{60}$, where the crystal structure changes from fcc to simple cubic (sc), occurs at 0.2 GPa at room temperature.[13,14] Furthermore, a second anomaly was reported at around 2 GPa in several experimental studies.[11,15–17] However, the values of the critical
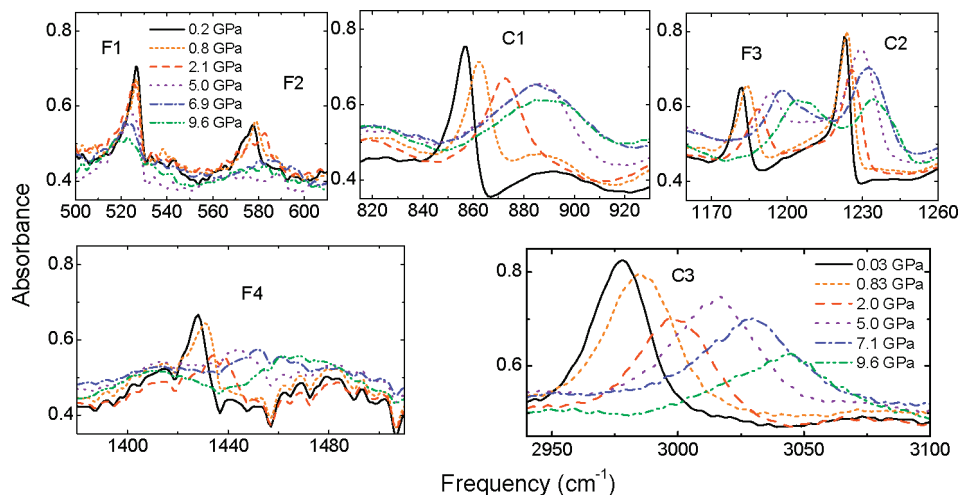
$C_{60} \cdot C_8H_8$ and $C_{70} \cdot C_8H_8$ Studied under Pressure

*J. Phys. Chem. C, Vol. 112, No. 45, 2008* **17527**



**Figure 2.** Absorbance spectra of $C_{60} \cdot C_8H_8$ in the mid-infrared frequency range for pressures up to 10 GPa. The vibrational modes of the fullerene (cubane) molecules are denoted by F (C).



**Figure 3.** Absorbance spectra of $C_{70} \cdot C_8H_8$ in the mid-infrared frequency range for pressures up to 10 GPa. The vibrational modes of the fullerene (cubane) molecules are denoted by F (C).
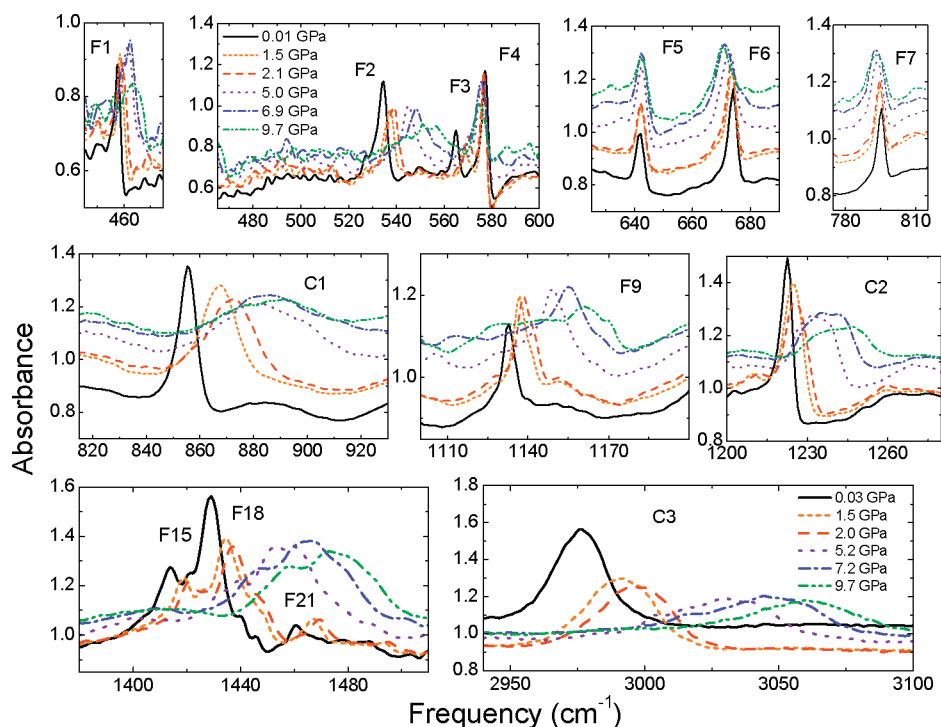
**TABLE 1: Frequencies of the Vibrational Modes of $C_{60} \cdot C_8H_8$ at Pressures ~0.5 and 4 GPa[a]**

| label | $\nu$ (cm$^{-1}$) at ~0.5 GPa | $\nu$ (cm$^{-1}$) at 4 GPa |
|-------|-------------------------------|----------------------------|
| F1 | 526 | 525 |
| F2 | 577 | 584 |
| C1 | 859 | 882 |
| F3 | 1182 | 1191 |
| C2 | 1223 | 1228 |
| F4 | 1429 | |
| C3 | 2980 | 3008 |

[a] The vibrational modes of the fullerene (cubane) molecules are denoted by F (C).

pressure of this second transition obtained by different experiments are not consistent, and the origin of this transition is still unclear. An increase in pressure is expected to have the same effect on a material as a decrease in temperature. Therefore, based on a comparison with the phase transitions occurring in $C_{60}$ with decreasing temperature—a transition to an orientationally ordered state at 260 K and a glass transition at 90 K—the two anomalies in $C_{60}$ at 0.2 and 2 GPa were attributed to an fcc-to-sc and a glass transition, respectively.[15,16]

In comparison, in $C_{60} \cdot C_8H_8$, an orientational ordering transition was found at 140 K at ambient pressure, where the rotational degrees of freedom of the fullerene molecules become restricted.[1,2] At this transition, the crystal structure of $C_{60} \cdot C_8H_8$ changes from fcc to orthorhombic.[1,2,10] In analogy to the $P-T$ phase diagram of $C_{60}$, we attribute the anomaly at 0.5 GPa to the occurrence of an orientational ordering of the fullerene molecules in $C_{60} \cdot C_8H_8$, accompanied by the pressure-induced transition from an fcc to orthorhombic crystal structure. This is in good agreement with the recent $P-T$ phase diagram based on the results from Raman and X-ray diffraction measurements under pressure.[6]

**TABLE 2: Frequencies of the Vibrational Modes of
$C_{70} \cdot C_8H_8$ at Pressures 0.4 and 4 GPa[a]**

| label | $\nu$ (cm$^{-1}$) at 0.4 GPa | $\nu$ (cm$^{-1}$) at 4 GPa |
|---|---|---|
| F1 | 458 | 460.6 |
| F2 | 535.4 | 542.6 |
| F3 | 565.8 | 575.2 |
| F4 | 577.1 | 576.6 |
| F5 | 641.8 | 642.2 |
| F6 | 673.8 | 672.7 |
| F7 | 795 | 793.7 |
| C1 | 857.7 | 867.2 |
| C | | 873.8 |
| C | | 890.1 |
| F8 | 1087.5 | 1101.0 |
| F9 | 1134.4 | 1145.6 |
| F10 | 1205.5 | 1220.2 |
| C2 | 1223.5 | 1225.2 |
| C | | 1229.5 |
| C | | 1234.3 |
| F11 | 1259 | |
| F12 | 1293 | |
| F13 | 1321.7 | |
| F14 | 1326.4 | |
| F15 | 1416.2 | 1425.2 |
| F16 | 1422.8 | 1428.5 |
| F17 | 1428.1 | 1434.6 |
| F18 | 1432.4 | 1437.3 |
| F19 | 1441.8 | 1445.2 |
| F20 | 1446.9 | 1453.4 |
| F21 | 1463 | 1470.5 |
| F | | 1480.3 |
| F22 | 1490 | 1502.9 |
| *F*23 | 1533 | |
| F24 | 1562.9 | 1575.2 |
| F25 | 1585.5 | 1583.7 |
| C3 | 2979.3 | 2998.6 |
| C | | 3017.2 |
| C | | 3030.5 |

[a] The vibrational modes of fullerene (cubane) are denoted by F (C).

In the fcc phase of $C_{60} \cdot C_8H_8$, the $C_{60}$ molecules rotate so fast that the distorting potential field of the surrounding molecules is averaged out. The cubane molecules occupy $O_h$ sites in these crystals, which is identical to the point group of the $C_8H_8$ molecule. This way no splitting is expected in the fcc phase. In the orthorhombic phase, on the other hand, the fullerene molecules are static. The highest possible site symmetry in orthorhombic $C_{60} \cdot C_8H_8$ is $D_{2h}$, and the irreducible representations of this point group are all one-dimensional. This means that splitting of both the $C_{60}$ and the cubane lines should be present. As one unit cell of the orthorhombic phase contains four inequivalent molecules of fullerene (and cubane), Davydov splitting should also be present. We did not observe any splitting up to the highest measured pressures, which means that the broadening due to the increase of pressure is larger than the magnitude of the splitting.

The anomaly at around 1.3 GPa cannot be assigned to the pressure-induced change of the orientational order in the $P-T$ phase diagram of pure $C_{60}$, since the orthorhombic structure precludes orientational disorder. Besides, due to the larger interfullerene distances in $C_{60} \cdot C_8H_8$, the significant interaction is that of fullerene–cubane rather than fullerene–fullerene. Therefore, this transition may have its origin in fullerene–cubane interactions. More indirect evidence for this assumption is that the infrared modes of cubane follow the same pressure dependence as the fullerene lines showing anomalies at the same pressure values.

According to our results, the vibrational modes in $C_{70} \cdot C_8H_8$ exhibit a stronger and fundamentally different pressure dependence than those in $C_{60} \cdot C_8H_8$. The cubane modes split into several lines at 0.8 and 1.75 GPa; at these pressures, there occurs a (less pronounced) change in the pressure dependence of the $C_{70}$ modes as well. At room temperature, the basic motion of the $C_{70}$ molecules is a uniaxial rotation around the long molecular axis ($C_5$).[1,2] This uniaxial rotation of the $C_{70}$ molecules might stop at around 0.8 GPa, in analogy with the pressure-induced orientational ordering in pristine $C_{70}$ at around 1 GPa.[18,19]

In the bct phase of $C_{70} \cdot C_8H_8$, the cubane molecules occupy axially elongated $O_h$ sites belonging to the $D_{4h}$ point group. In this point group, the $T_{1u}$ representations split into $A_{2u}$ and $E_u$, which are both infrared active. Consequently a two-fold splitting of the cubane lines should be already present at ambient pressure. The size of the splitting, however, is below the resolution of the measurements, indicating only a slight elongation of the $O_h$ site. $C_{70}$ is rotating in this phase, and we indeed do not see any splitting of its lines.

In the primitive monoclinic phase, the $C_{70}$ molecules are orientationally ordered with uniaxial motion, so splitting due to the lower site symmetry and the Davydov splitting can appear not only in the case of cubane, but also in the case of $C_{70}$ lines. The highest possible site symmetry in this phase is $C_{2h}$. As this point group has only one-dimensional representations, the $E_1'$ lines of $C_{70}$ are expected to split two-fold and the $T_{1u}$ lines of cubane 3-fold (see column a in Table 3). An additional two-fold Davydov splitting of all the modes is expected, as the unit cell now contains two inequivalent $C_{70}$ (and $C_8H_8$) molecules (see column b in Table 3). Of course, not all of the modes are infrared active. The number of these depends on the exact point groups appearing in the group theoretical derivation. If we consider all the possible cases of a primitive monoclinic $C_{70} \cdot C_8H_8$, there will be two possible splitting patterns appearing in the infrared spectrum; these are given in the third column of Table 3. The splitting of $C_{70}$ lines was not observed, but the cubane lines were indeed found to split with increasing pressure. It is interesting to note that the splitting of different $T_{1u}$ lines of cubane does not happen at the same pressures. The origin of the difference remains an open question.

An infrared absorption study on 1,4-dinitrocubane and cubane under pressure by Piermarini et al.[20] seems to be the only pressure-dependent experimental investigation on crystalline cubane. In this study, it was observed that cubane explodes spontaneously at room temperature at pressures above 3 GPa. This decomposition is the result of the considerable internal strain caused by the unusual 90° bond angles, rendering the cubane molecule more sensitive to the application of external pressure than fullerenes. As the cubane sublattice is already ordered, and there is no cubane–cubane contact, neither the orientational ordering calculated for the high-temperature phase of solid cubane[21] nor the bulk modulus estimation for the ordered phase[22] is relevant here; the principal factor determining the symmetry change is the ordering of the surrounding fullerene molecules.

As we have seen, the splitting of the lines predicted by group theory is usually obscured by the line width, the only exception being that of cubane in $C_{70} \cdot C_8H_8$ under pressure. This indicates the sensitivity of the cubane molecule to pressure, and stronger intermolecular interactions in $C_{70} \cdot C_8H_8$ than in $C_{60} \cdot C_8H_8$.

**3.2. Absorption Edge.** The molecular orbitals in van der Waals molecular crystals are broadened into bands due to intermolecular interactions at ambient conditions. The band
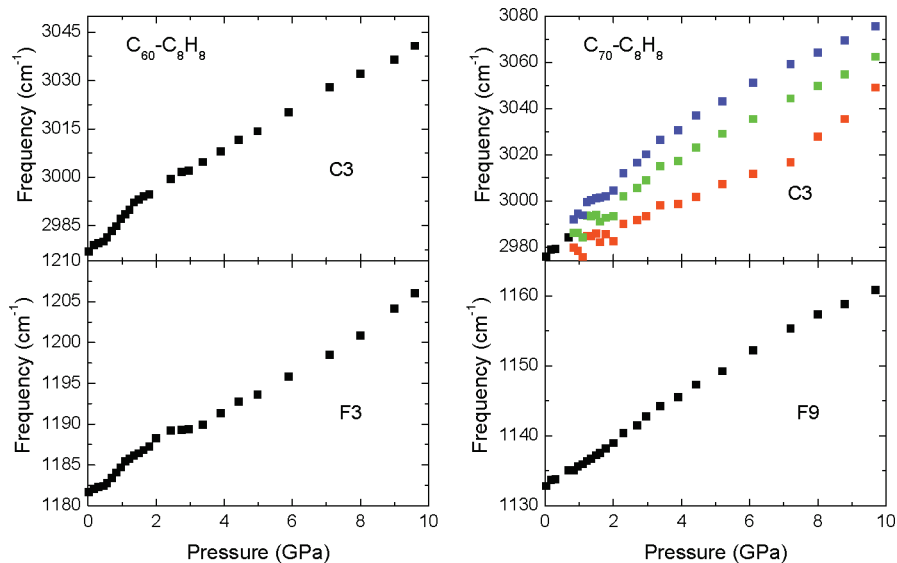
C$_{60}$·C$_8$H$_8$ and C$_{70}$·C$_8$H$_8$ Studied under Pressure

*J. Phys. Chem. C, Vol. 112, No. 45, 2008* **17529**



**Figure 4.** Pressure dependence of two selected vibrational modes of C$_{60}$·C$_8$H$_8$ and C$_{70}$·C$_8$H$_8$ plotted as a function of pressure up to 10 GPa. The vibrational modes of the fullerene (cubane) molecules are denoted by F (C); the labels are chosen in the order of increasing frequency.
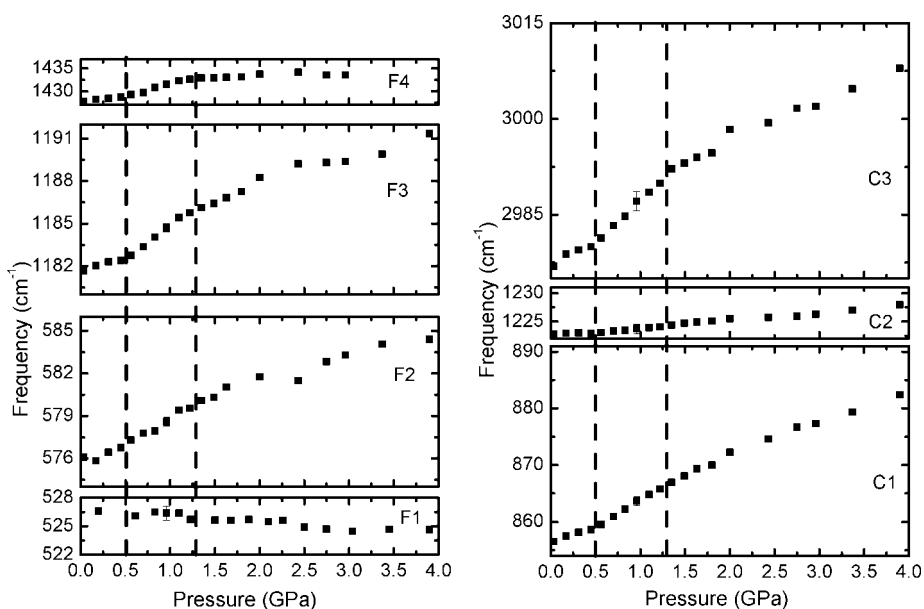


**Figure 5.** Frequencies of the vibrational modes of C$_{60}$·C$_8$H$_8$ plotted as function of pressure in the low pressure regime up to 4 GPa. The vibrational modes of the fullerene (cubane) molecules are denoted by F (C); the labels are chosen in the order of increasing frequency.

broadening and hence the onset of the electronic absorption are very sensitive to changes in intermolecular interactions. Therefore, the energy of the onset of the electronic absorption can serve as a measure of the strength of intermolecular interactions.

Both external and chemical pressure will affect the intermolecular distances. Via both ways, the importance of the intermolecular forces for the electronic properties can thus be clarified. In particular the application of external pressure is a "clean" way to continuously tune the intermolecular distances, and the effect on the absorption edge can be studied. Because of the enormous strength of the intramolecular bonds,[10] only minor effects due to possible pressure-induced distortions of the fullerene balls are to be expected, and therefore, we do not consider them in the following. (For the same reason, the pressure-induced redshift of the photoluminescence band and the absorption edge in the pure fullerite crystals C$_{60}$ and C$_{70}$, respectively, were attributed to the increasing intermolecular interactions only.)[29,30]

The absorption edge $E_a$ in C$_{60}$·C$_8$H$_8$ and C$_{70}$·C$_8$H$_8$ and its dependence on external pressure were determined from our transmittance spectra. Figure 7 shows the absorbance spectra of both compounds in the NIR−visible frequency range for selected pressures up to 10 GPa. The absorption strongly increases in this energy range due to the onset of the electronic excitations in fullerenes [cubane is transparent up to 50000 cm$^{-1}$ (see ref 23)]. For both compounds, the absorption edge shifts to lower energies on applying pressure. The absorption edge of C$_{70}$·C$_8$H$_8$ lies at a smaller energy and shows larger pressure-induced shifts compared to C$_{60}$·C$_8$H$_8$.

For a quantitative analysis, we considered the energy position where the absorbance changes its slope as a measure of the absorption edge. Accordingly, the first derivative of the absorbance shows a maximum (see inset of Figure 8 for illustration) whose position serves as an estimate of $E_a$. The energy position was determined by a Gaussian fit. The resulting pressure dependence of $E_a$ for C$_{60}$·C$_8$H$_8$ and C$_{70}$·C$_8$H$_8$ is shown in Figure
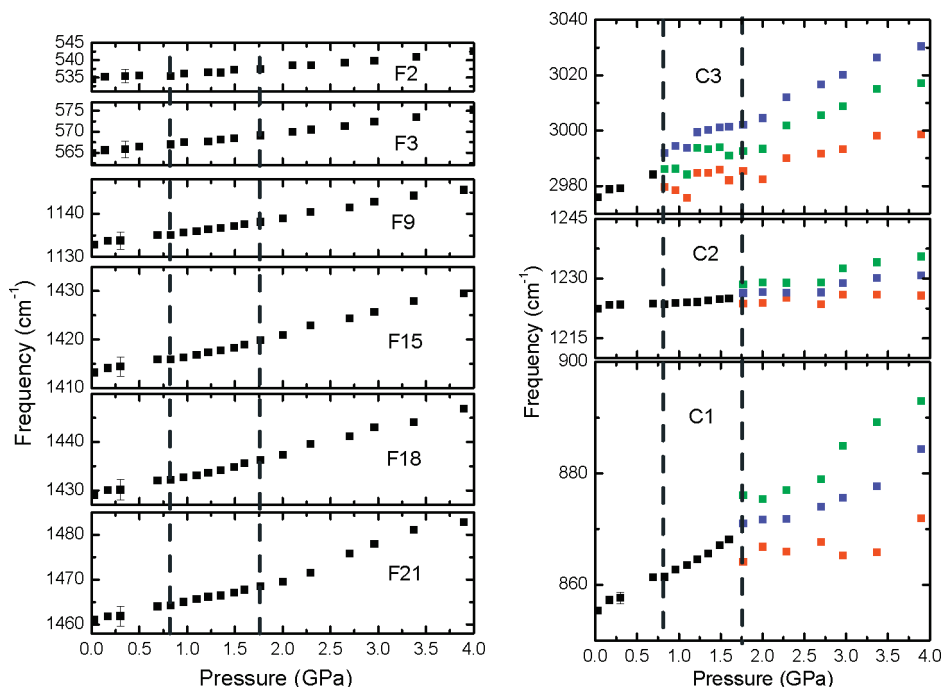
**Figure 6.** Frequencies of the vibrational modes of $C_{70} \cdot C_8H_8$ plotted as function of pressure in the low pressure regime up to 4 GPa. The vibrational modes of the fullerene (cubane) molecules are denoted by F (C); the labels are chosen according to Table 2. Only the fullerene modes with the largest pressure dependence are shown.

**TABLE 3: Splitting of the Originally Infrared Active Molecular Modes in the Primitive Monoclinic Phase of $C_{70} \cdot C_8H_8$ According to Group Theory: (a) the Number of Modes Arising Due to the Lower Site Symmetry; (b) the Number of Modes if We Take Davydov Splitting into Account, As Well; (c) the Number of Infrared Active Modes[a]**

|          |          | a | b | c |   |   |
|----------|----------|---|---|---|---|---|
| $C_{70}$ | $A_2''$  | 1 | 2 | 1 |   | 2 |
| $C_{70}$ | $E_1'$   | 2 | 4 | 2 | or | 4 |
| $C_8H_8$ | $T_{1u}$ | 3 | 6 | 3 |   | 6 |

[a] The two possible splitting patterns are associated with different possible factor groups and site symmetries in the primitive monoclinic system.

8. No anomalies are observed in contrast to the pressure dependence of the vibrational modes presented above. The results were rechecked using argon as pressure transmitting medium, in order to rule out possible nonhydrostatic effects. According to Figure 8 the values of $E_a$ for the different pressure media agree reasonably well.

The dependence of $E_a$ on pressure $P$ is nonlinear and could be perfectly described by a second-order polynomial $E_a(P) = E_a(0) + d_1P + d_2P^2$. The so-obtained fitting parameters are $E_a(0) = 1.84$ eV (1.77 eV), $d_1 = -0.055$ eV $GPa^{-1}$ ($-0.065$ eV $GPa^{-1}$), and $d_2 = 0.0015$ eV $GPa^{-2}$ (0.0018 eV $GPa^{-2}$) for $C_{60} \cdot C_8H_8$ ($C_{70} \cdot C_8H_8$). The nonlinear shift is analogous to that found in pristine $C_{60}$ and $C_{70}$,[10,24,25] and the parameter $d_1$ for $C_{60} \cdot C_8H_8$ is comparable to that observed by Meletov et al.[26−28] for the 1.7 eV threshold at low pressure.

We furthermore studied the effect of the chemical pressure on the electronic properties of $C_{60} \cdot C_8H_8$ and $C_{70} \cdot C_8H_8$ by a comparison with other fullerene-based materials regarding the absorption edge $E_a(0)$ and interfullerene distance. In Table 4, we list our results together with those for the pristine fullerenes and fullerene clathrates. The absorption threshold values for the other fullerene-derived compounds were determined by the same procedure described above, in order to be comparable. The size
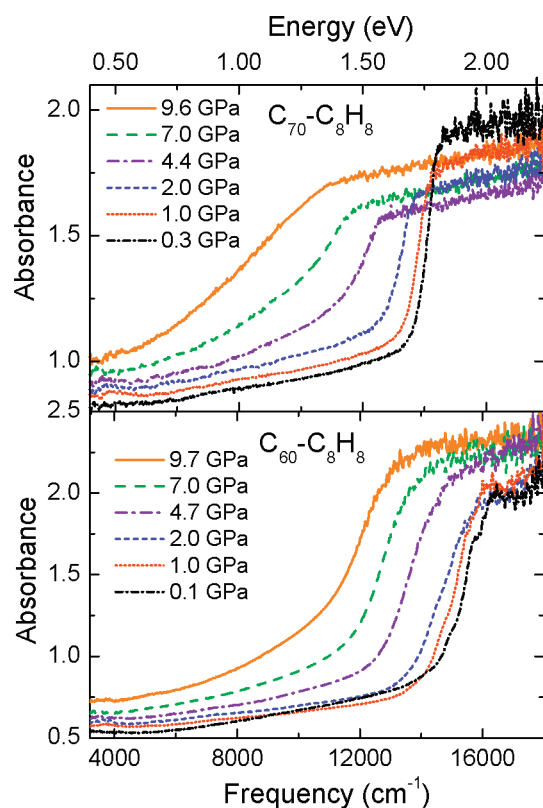


**Figure 7.** Absorbance spectra of $C_{60} \cdot C_8H_8$ and $C_{70} \cdot C_8H_8$ in the NIR to visible frequency range are shown for selected pressures between 0 and 10 GPa, using KCl as pressure transmitting medium.

of $E_a(0)$ for $C_{60} \cdot C_8H_8$ is significantly larger than for pure solid $C_{60}$.[10,24,28,29] A similar blueshift of the absorption edge compared to pure $C_{60}$ was observed for the $C_{60}$ clathrates.[31] Here it was argued that the blueshift results from the increase in molar volume, leading to a decrease in the molecular overlap between the $C_{60}$ molecular orbitals: the guest molecules in the clathrates
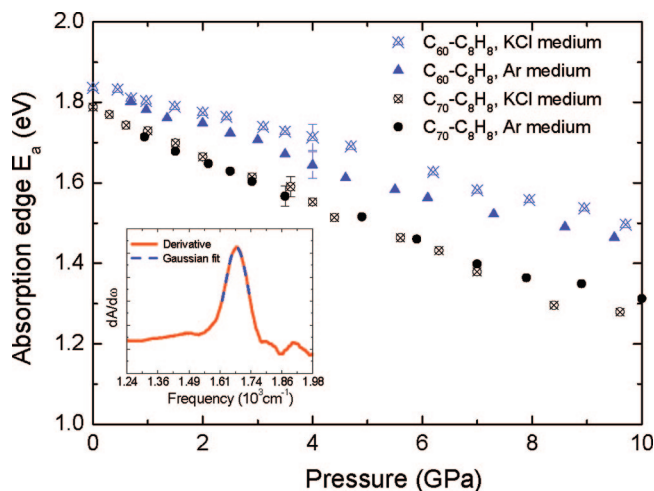
$C_{60} \cdot C_8H_8$ and $C_{70} \cdot C_8H_8$ Studied under Pressure

*J. Phys. Chem. C, Vol. 112, No. 45, 2008* **17531**



**Figure 8.** Absorption edge $E_a$ of $C_{60} \cdot C_8H_8$ and $C_{70} \cdot C_8H_8$ obtained from transmittance measurements using KCl and Ar as pressure transmitting media plotted as a function of pressure. The inset shows, as an example, the derivative of the absorbance measured at 1.5 GPa with respect to frequency, $dA/d\omega$; the energy position of the maximum, as determined from a Gaussian fit (dashed line), served as an estimate for the size of $E_a$.

**TABLE 4: Ambient-Pressure Absorption Edge $E_a(0)$ and Average Interfullerene Distance in Various Fullerene-Based Materials[10,18,24,28−37]**

| compound | $E_a(0)$ (eV) | intermolecular distance (Å) |
|---|---|---|
| $C_{60}$ | 1.73 | 10.01 |
| $C_{60}$-clathrates | 1.81 | $\approx 10.1$ |
| $C_{60} \cdot C_8H_8$ | 1.84 | 10.42 |
| $C_{70}$ | 1.79 | 10.61 |
| $C_{70} \cdot C_8H_8$ | 1.77 | 10.88 |

simply act as spacers, causing a lattice expansion, and no interaction is present between the host and guest molecules. A similar argument might hold in the case of $C_{60} \cdot C_8H_8$, but despite the much larger interfullerene distance than that in clathrates,[2] the absorption edge does not differ much from that in the clathrates. We regard this fact as evidence for the attractive fullerene−cubane molecular recognition[3] increasing the orbital overlap and thereby counteracting the spacer effect. Recent band-structure calculations[38] indeed raised the possibility of hybridization between cubane and $C_{60}$, which would have as a consequence the increase in heteromolecular overlap. It seems that in $C_{70} \cdot C_8H_8$ these two contributions nearly cancel each other, since no significant shift of the absorption edge compared to pristine $C_{70}$ is observed. $C_{70} \cdot C_8H_8$ having a more effective space filling than $C_{60} \cdot C_8H_8$ explains the increased molecular recognition interaction which leads to both smaller increase in intermolecular distance and no shift (in fact, a slight redshift) in the absorption edge.

## 4. Conclusions

Pressure-dependent transmittance measurements over a broad frequency range (infrared to visible) on $C_{60} \cdot C_8H_8$ and $C_{70} \cdot C_8H_8$ reveal pressure-induced phase transitions and give an insight into the nature of interactions in this new class of rotor-stator compounds. The pressure dependence of the vibrational modes in $C_{60} \cdot C_8H_8$ shows anomalies at 0.5 and 1.3 GPa, the first of which we assign to a pressure-induced orientational ordering transition of the fullerene molecules; the second anomaly is probably correlated with fullerene−cubane interactions. According to the pronounced pressure-induced changes of the

vibrational modes, the cubane molecules in $C_{70} \cdot C_8H_8$ are more sensitive to the application of pressure than in $C_{60} \cdot C_8H_8$, reflecting the stronger molecular recognition interactions in $C_{70} \cdot C_8H_8$ due to more effective space filling. The cubane modes exhibit pressure-induced splittings into several lines at 0.8 and 1.75 GPa, which we interpret in terms of symmetry changes in the cubane molecules induced by distortions.

From our transmittance data in the near-infrared to visible frequency range, we could follow the energy of the absorption threshold in $C_{60} \cdot C_8H_8$ and $C_{70} \cdot C_8H_8$ as a function of pressure. For both compounds, the threshold shifts to lower energies with increasing pressure due to an increasing overlap of the molecular orbitals, and the pressure dependence can be described by a second-order polynomial. The absorption threshold of $C_{60} \cdot C_8H_8$ is larger than that of pristine $C_{60}$ but less than expected based on intermolecular distance, indicating that the cubane molecules do not simply act as spacers reducing the overlap of the $C_{60}$ molecular orbitals, but heteromolecular overlap caused by molecular recognition plays a role as well. In $C_{70} \cdot C_8H_8$, practically no shift of the optical absorption edge is observed, in agreement with the enhanced molecular recognition interactions compared to $C_{60} \cdot C_8H_8$.

## References and Notes

(1) Pekker, S.; Kováts, É.; Oszlányi, G.; Bényei, G.; Bortel, G.; Jalsovszky, I.; Jakab, E.; Borondics, F.; Kamarás, K.; Bokor, M.; Kriza, G.; Tompa, K.; Faigel, G. *Nat. Mater.* **2005**, *4*, 784.
(2) Bortel, G.; Faigel, G.; Kováts, É.; Oszlányi, G.; Pekker, S. *Phys. Stat. Sol B* **2006**, *243*, 2999.
(3) Pekker, S.; Kováts, É.; Oszlányi, G.; Bényei, G.; Klupp, G.; Bortel, G.; Jalsovszky, I.; Jakab, E.; Borondics, F.; Kamarás, K.; Faigel, G. *Phys. Stat. Sol B* **2006**, *243*, 3032.
(4) Kuntscher, C. A.; Frank, S.; Kamarás, K.; Klupp, G.; Kováts, É.; Pekker, S.; Bényei, G.; Jalsovszky, I. *Phys. Stat. Sol. B* **2006**, *243*, 2981.
(5) Iwasiewicz-Wabnig, A.; Sundqvist, B.; Kováts, É.; Jalsovszky, I.; Pekker, S. *Phys. Rev. B* **2007**, *75*, 024114.
(6) Sundqvist, B.; Iwasiewicz-Wabnig, A.; Kováts, É.; Pekker, S. *Mater. Res. Symp. Proc.* **2007**, *987*, PP03−04.
(7) Klupp, G.; Borondics, F.; Kováts, É.; Pekker, Á.; Bényei, G.; Jalsovszky, I.; Hackl, R.; Kamarás, K.; Pekker, S. *J. Phys. Chem. B* **2007**, *111*, 12375.
(8) Huber, G.; Syassen, K.; Holzapfel, W. B. *Phys. Rev. B* **1977**, *15*, 5123.
(9) Mao, H. K.; Xu, J.; Bell, P. M. *J. Geophys. Res. [Atmos.]* **1986**, *91*, 4673.
(10) Sundqvist, B. *Adv. Phys.* **1999**, *48*, 1.
(11) Huang, Y.; Gilson, D. F. R.; Butler, I. S. *J. Phys. Chem.* **1991**, *95*, 5723.
(12) Yamawaki, H.; Yoshida, M.; Kakudate, Y.; Usuba, S.; Yokoi, H.; Fujiwara, S.; Aoki, K. *J. Phys. Chem.* **1993**, *97*, 11161.
(13) Samara, G. A.; Hansen, L. V.; Assink, R. A.; Morosin, B.; Schirber, J. E.; Loy, D. *Phys. Rev. B* **1993**, *47*, 4756.
(14) Schirber, J. E.; Kwei, G. H.; Jorgensen, J. D.; Hitterman, R. L.; Morosin, B. *Phys. Rev. B* **1995**, *51*, 12014.
(15) Meletov, K. P.; Christofilos, D.; Kourouklis, G. A.; Ves, S. *Chem. Phys. Lett.* **1995**, *236*, 265.
(16) Meletov, K. P.; Christofilos, D.; Ves, S.; Kourouklis, G. A. *Phys. Rev. B* **1995**, *52*, 10090.
(17) Jeon, S. -J.; Kim, D.; Kim, S. K.; Jeon, I. C. *J. Raman Spectrosc.* **1992**, *23*, 311.
(18) Kawamura, H.; Kobayashi, M.; Akahama, Y.; Shinohara, H.; Sato, H.; Saito, Y. *Solid State Commun.* **1992**, *83*, 563.
(19) Kawamura, H.; Akahama, Y.; Kobayashi, M.; Shinohara, H.; Sato, H.; Saito, Y.; Kikegawa, T.; Shimomura, O.; Aoki, K. *J. Phys. Chem. Solids* **1993**, *54*, 1675.

(20) Piermarini, G. J.; Block, S.; Damavarapu, R.; Iyer, S. *Prop. Expl. Pyro.* **1991**, *16*, 188.

(21) Murugan, N. A. *J. Chem. Phys.* **2005**, *123*, 244514.

(22) Yildirim, T.; Ciraci, S.; Kilic, C.; Buldum, A. *Phys. Rev. B* **2000**, *62*, 7625.

(23) Eaton, P. E. *Angew. Chem., Int. Ed. Engl.* **1992**, *311*, 1421.

(24) Snoke, D. W.; Syassen, K.; Mittelbach, A. *Phys. Rev. B* **1993**, *47*, 4146.

(25) Sundqvist, B. *Phys. Stat. Sol. B* **2001**, *223*, 469.

(26) Meletov, K. P.; Dolganov, V. K.; Zharikov, O. V.; Kremeenskaya, I. N.; Ossipyan, Yu. A. *J. Phys. Paris* **1992**, *2*, 2097.

(27) Meletov, K. P.; Kourouklis, G. A.; Christofilos, D.; Ves, S. *J. Exp. Theoret. Phys.* **1995**, *81*, 798.

(28) Meletov, K. P.; Christofilos, D.; Ves, S.; Kourouklis, G. A. *Phys. Stat. Sol. B* **1996**, *198*, 553.

(29) Sood, A. K.; Chandrabhas, N.; Muthu, D. V. S.; Jayaraman, A.; Kumar, N.; Krishnamurthy, H. R.; Pradeep, T.; Rao, C. N. R. *Solid State Commun.* **1992**, *81*, 89.

(30) Meletov, K. P.; Dolganov, V. K.; Ossipyan, Yu. A. *Solid State Commun.* **1993**, *87*, 639.

(31) Kamarás, K.; Breitschwerdt, A.; Pekker, S.; Fodor-Csorba, K.; Faigel, G.; Tegze, M. *Appl. Phys. A: Mater. Sci. Process.* **1993**, *56*, 231.

(32) Pekker, S.; Faigel, G.; Fodor-Csorba, K.; Gránásy, L.; Jakab, E.; Tegze, M. *Solid State Commun.* **1992**, *83*, 423.

(33) Pekker, S.; Faigel, G.; Oszlányi, G.; Tegze, M.; Kemény, T.; Jakab, E. *Synth. Met.* **1993**, *55−57*, 3014.

(34) Krätschmer, W.; Lamb, L. D.; Fostiropoulos, K.; Huffmann, D. R. *Nature* **1990**, *347*, 354.

(35) Heiney, P. A.; Fischer, J. E.; McGhie, A. R.; Romanow, W. J.; Denenstein, A. M.; McCauley, Jr, J. P.; Smith III, A. B.; Cox, D. E *Phys. Rev. Lett.* **1991**, *66*, 2911.

(36) Jiang, L.; Li, J.; Nagahara, L. A.; Kino, N.; Kitazawa, K.; Iyoda, T.; Hashimoto, K.; Fujishima, A. *Appl. Phys. A: Mater. Sci. Process.* **1995**, *61*, 17.

(37) Oh, D. -H.; Lee, Y. H. *Phys. Rev. Lett.* **1995**, *75*, 4230.

(38) Zólyomi, V.; Koltai, J.; Kürti, J.; Pekker, S. *Phys. Rev. B*, submitted for publication.